QFL AND LITHO FACIES: PREDICTING RESERVOIR QUALITY OF THE MIDDLE MIOCENE DEEP-WATER FACIES AT KUTEI AND NORTH MAKASSAR BASINS

QFL DAN FASIES BATUAN: PREDIKSI KUALITAS RESERVOIR FASIES LAUT DALAM BERUMUR MIOSEN TENGAH DI CEKUNGAN KUTEI DAN MAKASSAR UTARA

Kuntadi Nugrahanto[1,2], Ildrem Syafri[1], and Budi Muljana[1]

[1] Postgraduate Program, Faculty of Geological Engineering, the University of Padjadjaran

[2] Upstream Subholding Pertamina Hulu Energi (PHE)

Corresponding author: kuntadi19001@mail.unpad.ac.id; kuntadi.nugrahanto@pertamina.com

(Received 21 June 2021; in revised form 16 June 2021; accepted 08 July 2021)

ABSTRACT: As it is widely known the oil and gas wellbores offshore Kutei and North Makassar have not optimally penetrated the objective strata, which is the Middle Miocene's deep-water reservoirs. Therefore, evaluating the quality of these reservoirs with onshore dataset then comparing them with the proven Late Miocene's deep-water producing reservoirs had been very fundamental. The study focuses on the assessment of QFL (Quartz, Feldspar and Lithic fragments) and sandstones litho-facies based on the rock samples from conventional-core and side-wall core, and well-logs data from forty wells onshore and offshore. These rock samples are bounded by the key biostratigraphy intervals of M40M33, M45M40, M50M45 (Middle Miocene), and M65M50, M66M65, M70M66, M80M70 (Late Miocene). Subdivisions of the reservoirs considered the sandstone litho facies, NTG ratio, sorting, and grain size, to come up with five groups in the Middle Miocene deltaic facies: FLU_SX, DC_SX, DC_SM, DC_SM, and DF_SC; and four groups in the Late Miocene deep-water facies: SSWS, MSWS, SSPS, and MSPS. Core-based porosity and permeability further explain the relationship between the reservoir quality with the sandstones' composition and litho facies, and concluded that high-energy depositional system is mainly associated with the FLU_SX, DC_SX, SSWS and MSWS being the reservoir with best quality. Oppositely, the DF_SC, SSPS, and MSPS are classified the reservoir with worst to none quality. A cross plot between core-based porosity and maximum burial depth is able to postulate the relational trend of decreasing reservoir quality with deeper depth.

Keywords: Middle Miocene, deep water, QFL, litho facies, Kutei, North Makassar

ABSTRAK: *Telah umum diketahui bahwa sumur bor minyak dan gas di lepas pantai Kutei dan Makassar Utara belum secara optimal menembus reservoir fasies laut dalam berumur Miosen Tengah, yang merupakan obyektif utama dalam penelitian ini. Oleh karenanya penulis melakukan studi banding antara reservoir obyektif yang umumnya berlokasi di daratan dengan reservoir berumur Miosen Atas yang telah terbukti memproduksi hasil migas di lepas pantai laut dalam. Fokus studi ini adalah melakukan pengkajian komposisi QFL (fragmen Kuarsa, Felsfar dan Litik) dan fasies batuan batupasir berdasarkan sampel batuan yang diambil dari data inti batuan (core) dan data dinding bor (side-wall core), serta data log elektrik yang berasal dari sekitar empat puluh buah sumur. Sampel batuan ini dibatasi oleh marker biostratigrafi: M40M33, M45M40, M50M45 (Miosen Tengah), dan M65M50, M66M65, M70M66, M80M70 (Miosen Akhir). Fasies reservoir dapat dikenali berdasarkan fasies batuan batupasir, rasio NTG, sortasi, dan ukuran butir terutama pada fasies delta berumur Miosen Tengah: FLU_SX, DC_SX, DC_SM, DC_SM, dan DF_SC, dan untuk fasies laut dalam Miosen Akhir: SSWS, MSWS, SSPS, dan MSPS. Selanjutnya porositas dan permeabilitas yang diukur pada batuan inti bor tersebut dapat digunakan untuk menerangkan hubungan antara kualitas reservoir dengan komposisi batupasir maupun fasies batuan. Sistem pengendapan berenergi tinggi terutama yang berhubungan dengan fasies batuan FLU_SX, DC_SX, SSWS dan MSWS merupakan reservoir dengan kualitas terbaik; dan fasies batuan DF_SC, SSPS, dan MSPS kebalikannya. Hubungan antara porositas berbasis data inti batuan dengan kedalaman (depth of burial) secara umum dapat menggambarkan pola penurunan kualitas reservoir seiring bertambahnya kedalaman.*

Kata Kunci: *Miosen Tengah, laut dalam, QFL, fasies batuan, Kutai, Makassar Utara*

INTRODUCTION

Kutei basin is one of the major hydrocarbon basins in Indonesia with multi-billions barrel reserves of oil equivalent (bboe) have been discovered to date. More than 8.0-km thick sediment has been deposited in the basin where the thickest is reached around the modern-day Mahakam delta (after Hall & Nichols, 2002; in Witts et al., 2015). The study area includes the onshore and offshore parts of the Kutei and north Makassar basins (Figure 1). After the last big discoveries of the "classical" middle-to-late Miocene deltaic play; Sisi and NW Peciko (Duval, 1992), the sequence-stratigraphic concept was applied to delineate more hydrocarbon reserves in the late Miocene-to-Pliocene deep-water play.

To prove the concept, Unocal Indonesia initiated the SX deep-water drilling technology and pioneered a back-to-back drilling campaign along the modern-day deep-water slope during the 1996-to-2005 (Unocal Indonesia Exploration and Drilling Team, 2016; in Nugrahanto et al., 2021). Several deep-water wells, including the discovery ones had confirmed the deltaic progradation easterly from Miocene to Recent intervals, however most of the middle Miocene deep-water play remains unpenetrated. The integration of seismic stratigraphy, core-log facies description, and petrology data had been integrated to correlate and describe the relationship between sedimentary rate and facies, with the mineral composition at different ages. The aim of the study is to classify the clusters of quartz, feldspar, and lithic fragments (QFL) composition with respect to the reservoir age, and qualitative reservoir quality of the middle Miocene as the focus of the study, to the late Miocene reservoirs to be compared with.

The study area is tectonically situated on the continental crust that accreted to the Sundaland during the Cretaceous to Cenozoic, and is side-by-side with several continental blocks derived from the Gondwanaland such as Mangkalihat, West Sulawesi, Paternoster, and southwest Borneo in the late Triassic to late Jurassic (Metcalf, 2011 and 2013; Hall and Sevastjanova, 2012). Several key major tectono-stratigraphic events in the study area are:

1) The results of Zircon U-Pb dating conducted in the Oligocene and early Miocene rock samples at Barito Basin (Witts *et al*., 2014), and the same dating from the insitu diorite porphiry at Lamandau (Shuang Li *et al*., 2015), both suggested the latest plate-tectonic related volcanisms in the Borneo was recorded at the Late Cretaceous of 82-70 Ma.

2) The South China Sea rifting opened in the Eocene-Oligocene and triggered movement of the Luconia Continent to the southeast direction. It led part of the South China Sea Plate subducted beneath the Sundaland. Due to the opening of South China Sea Plate, the Luconia

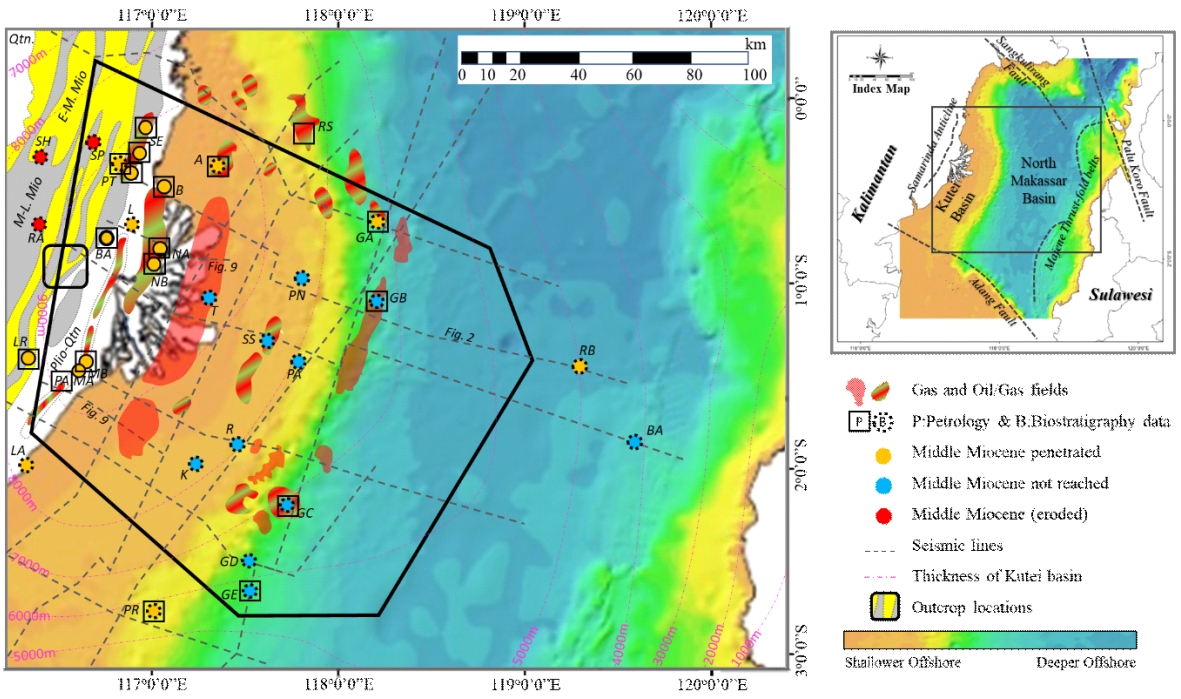

Figure 1. It shows simplified surface geological map (modified *from* Supriatna *et al*., 1995), hydrocarbon fields, well symbols, 2D seismic lines, Kutei sedimentary isopach, and water depth. Black rectangle is the study area. Index map shows the major bounding faults (*from* Nugrahanto *et al*., 2021)

continental crust had collided and docked onto the northern tip of of the Sundaland during the Middle Oligocene (Daines, 1985 and Hutchison, 1996; both *in* Soeria-Atmadja *et al*., 1999). The curvature suture of this collision is associated with the the Lupar Line where the imbricated ophiolites are found. The Late Eocene to Oligocene sag-related deep-to-shallow marine fine-grained materials deposited in a large embayment paleogeography (Morley and Morley, 2013; *in* Hall, 2013). This sub-regional sag was potentially associated with the ~35^{o} counter-clock wised (CCW) Borneo rotation (Advokaat *et al*., 2018).

3) As the subsidence gradually ceased by Late Oligocene, back-stepping reefal carbonates developed over the syn-depositional highs along the southern and northern edges of the Kutei Basin (van de Weerd *et al*., 1987; *in* Saller and Vijaya, 2002).

4) Early Miocene uplift and erosion along with the initiation of huge clastics progradation (Chambers and Daley, 1995; *in* Werdaya *et al*., 2017) had resulted in the proto Mahakam deltaic succession until the Late Miocene towards the present day, easterly (Moss and Chambers, 1999; *in* Werdaya *et al*., 2017). This contractional event is interpreted due to another ~10^{o} counter-clockwise Borneo rotation (Advokaat *et al*., 2018).

5) The prograded deltaic systems reached its highest sedimentation rate in Middle Miocene, known Middle Miocene Unconformity (MMU) that corresponds to the VIM 58-59, and up to the earliest late Miocene that fits with the VIM 62-64 (Morley *et al*., 2016).

6) Pliocene compressional event had emerged the West Sulawesi highlands to expose and erode the Mamasa granitoid then transported it into the deep-water Kutei Basin until the Recent. At the same time, N-S trend Samarinda Anticlinorium had been formed (Moss *et al*., 1997).

METHODS AND MATERIALS

Seismic-sequence stratigraphy

Basic concept of sequence stratigraphy is applied as it discusses rocks relationships in a chronostratigraphic framework of repetitive, genetically-related strata bounded by either erosional surfaces, hiatus, or correlative conformable stratas (Wagoner *et al*., 1988; *in* Nugrahanto *et al*., 2021). Lowstand, transgressive, and highstand system tracts (LST, TST, HST) are described based on the parasequence-sets. The most important system tract to notice is the type-1 sequence boundary (LST) that seismically may indicate forced-regressive shelf breaks (Posamentier, 2004; *in* Nugrahanto *et al*., 2021). At the same time, it can generate incised-valley erosional shape to deliver clastics deposits further into the slope break and basin floor during significant fall of relative sea-level.

The other alternative would be a gravity-driven mechanism at the down-slope along the sub-marine shelf margin was introduced by Shanmugam (2013, 2015, 2017) as the reasonable process in transporting the gravel to coarse-grained clastics into the slope and basin floor settings. The process includes debris flow, slump, and slide.

Integrating the outcrops, wells, and 2D seismic data are essential to generate the chronostratigraphic chart, isopach maps, and gross depositional environment (GDE) maps (Nugrahanto *et al*., 2021). These are able to define the depositional trends onshore and offshore.

Sedimentary-rock petrology

The tectonic setting of the provenance may contribute to the clastic-rocks composition (Dickinson and Suczek, 1979; *in* Tanean, 1994) and the sedimentary evolution that corresponds to the morphology gradient, depositional environments, distance between the hinterland to basin, subsidence rate, and weathering potential (Heins *et al*., 2007). The long process of transportation and sedimentation through the Proto Mahakam's fluvio-deltaic drainage systems toward the deep-water setting of north Makassar Basin become important aspect to indicate. The massive sediment transport through the incised valleys (IV) during periodic relative sea-level drops is thought to be inline with high-sedimentation rates. During the transportation process, the rocks went through the grain sorting, changed in the grain size and shape, until the post-sedimentation processes of burial compaction and at the same time depressed and exposed to the high temperatures (Tanean *et al*., 1996).

To extend the author's previous publication on the Early Miocene's rock samples *in* Werdaya *et al*. (2017), this study focuses to the Middle Miocene's petrography dataset taken from point-count analysis at the conventional core and side-wall core data. In addition to the previous well data, this study has added the other data points onshore-transition areas from Tanean (1994) and Tanean *et al*. (1996), as well as ten additional wellbores located offshore Kutei and deep-water North Makassar (Corelab, 2003). It is important to notice that various petrographers and service contractors, who had looked at the onshore and offshore dataset may apply different level of detail in their mineralogical descriptions.

This study will qualitatively predict the reservoir quality at the Middle Miocene's deep-water interval using

quartz, feldspar, and lithics (QFL) ternary diagram introduced by Folk (1988; *in* Aryati *et al*., 2019). The QFL generally demonstrates the sedimentary-source provenance, as well as the dominant composition of quartz minerals relative to the lithics and feldspars that have mainly related to the depositional facies. The rigid minerals comprise the lithics and feldspar components, while the ductile minerals consist of chert and clay minerals. Both minerals correspond to non-reservoir components as they have been very sensitive to the depth of burial (Werdaya *et al*., 2017). For the purpose of exhibiting the reservoir quality, the authors only utilize the porosity and permeability data from conventional core data.

RESULTS

Sub-regional Structure Geology and Depositional System

A schematic cross section was generated using the west-northwest to east-southeast (WNW-ESE) 2D seismic composite lines at the northern portion of the study area. The seismic-biostratigraphy correlation of the "M" markers had been carefully correlated to the sedimentation rates (Morley *et al*., 2016; *in* Nugrahanto *et al*., 2021). This section shows an overal prograding package with potential incised-valley (IV) features easterly. The western tip of the cross section structurally suggests a general trend of south-southwest to north-northeast (SSW-NNE) high-relief and tight inverted-fold belts that shifted into lower-relief and wider folds toward the present-day deep-water slope. It finally changes into much lower-to-no relief structure into the deep-water setting at the eastern tip of the study area (Figure 2).

The isopach maps within the "M markers" are utilized in generating several GDE maps (Figure 3) despite of the limitation of middle Miocene data points and seismic quality offshore deep water (Nugrahanto *et al*., 2021). Proto Mahakam River; red color in Figure 4 has been believed the paleo-drainage system in the Upper and Lower Kutei Basins covering the onshore areas such as Nyaan, Muyup, Kelian, Muara Wahau, Busang, and continues to the offshore depositional settings into the study area. Thicker isopach in Figure 3 shows the potential paleo-drainage systems that may represent incised-valley (IV) fill as well as sedimentary pods in the deltaic into the shallow marine environments. It established the potential clastic-reservoir filled into the slope and basin floor settings of the deep-water environment. Thinner isopach more easterly relates to the distal and / or condensed sections throughout the deep-water region.

QFL Composition

Previous analyses at mainly onshore petrographic samples throughout the delta to marine facies of the early-to-late Miocene's sediments provided four apparent petrologic subdivisions (Tanean, 1994 and Tanean *et al*., 1996): 1) the early Miocene's sediment (23-17 Ma), which was older than the M33 marker had moderate quartz and lithic components but high in volcanic-lithic components, 2) the latest early Miocene to the earliest Middle Miocene's sandstones (17-14.5 Ma) that nearly correlated to the M40-M33 zone were dominantly volcanogenic, 3) Middle to Late Miocene's sandstones, the equivalent to the M40-M65 zone, were highly composed by quartz with non-associated volcanic minerals, and finally 4) the Pliocene to Recent sandstones were similar to the type-2 (volcanogenic). All rock samples were the recycled orogen dominated by the lithic components that gradually changed to quartz dominant towards the younger-age formations.

Samples in this study come from twenty-nine onshore wells at the SE, PT, B, NA, NB, BA, MA, MB, and PA fields, and offshore wells at the A, RS, GA, GB, GC, GE, and PR fields (Figure 1) represent the deltaic to

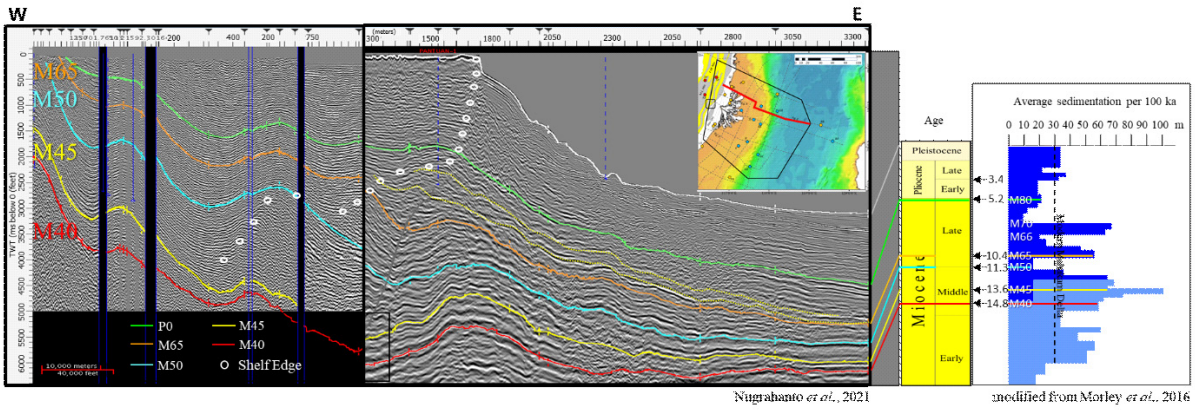

Figure 2. A 2D-seismic composite line showing "M" markers in prograding succession with Miocene's stratigraphic column and average sedimentation rates (modified from Nugrahanto *et al.,* 2021).

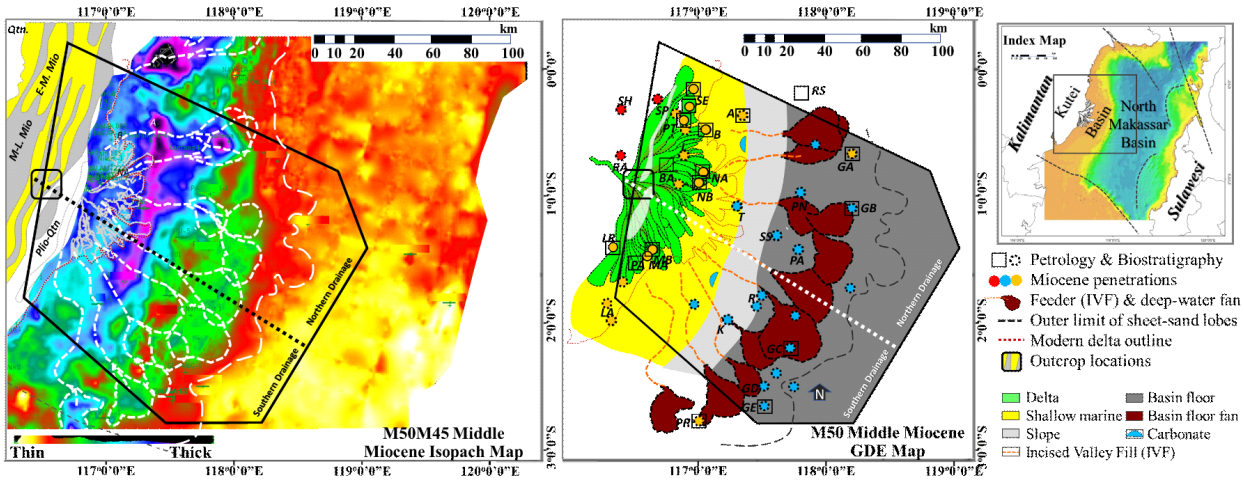

Figure 3. M45-M50 isopach maps (left) showing the paleo-drainage patterns, and a GDE map (Nugrahanto *et al.*, 2021) of its uppermost part of the M45-M50 (right) illustrating the northern and southern drainage systems.

deep-marine depositional settings of the Kutei and North Makassar Basins (Figures 1 and 4). The QFL plot of the Middle to Late Miocene clastics shows that the samples mainly lie along the litharenitic trend on the right side of the ternary diagram. The remaining samples are located along the arkosic trends as shown on the left-hand side of the ternary diagram (Figure 4).

The Cretaceous-age rocks exposed along the Sibu-Rajang Accretionary Prism is interpreted to be the sedimentary provenance for the Early Miocene's (N4-N7 or older than the younger section that equivalent to the M40M33 (N8A-early N10), volcanogenic sandstones were defined since the volcanic-lithic fragments in it increased from the average of <10% to >20% of the framework grains (Tanean *et al.*, 1996). The overall Middle Miocene sections (M40-M50 or N10-N14) was categorized high-quartzose sandstones as they have an average of >80% of the framework grains (Tanean *et al.*, 1996; and Figure 5 in this study, 2021). The Middle Miocene's (M50M45 and M45M40) and the lower part of Late Miocene's sam-

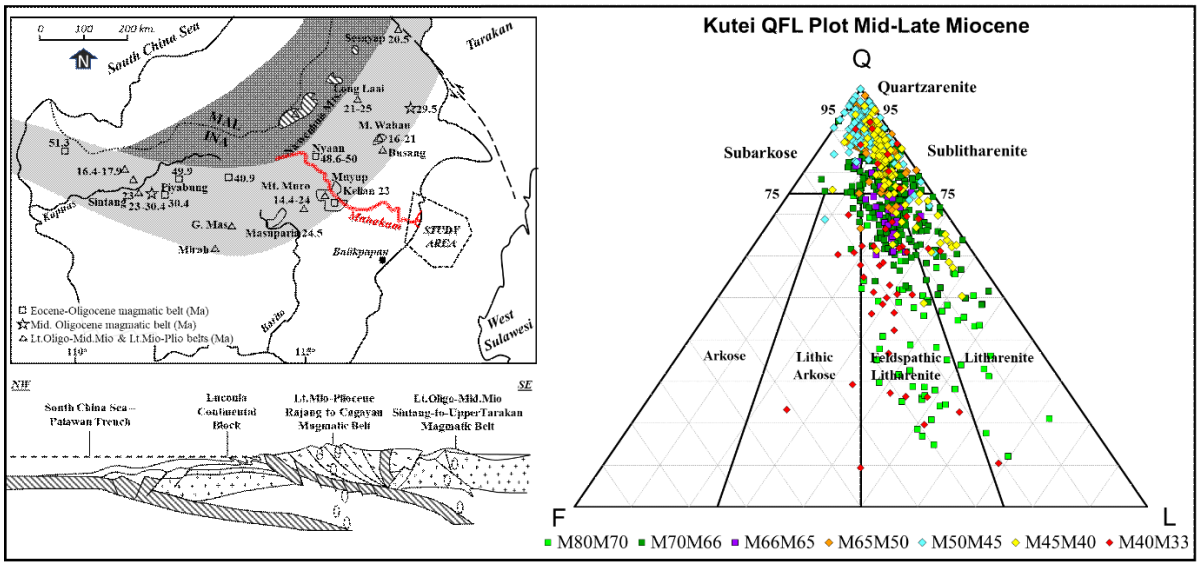

Figure 4. A NW-SE section and basemap showing the dark-grey and light-grey polygons, which are the magmatic belt of Late Oligocene to Middle Miocene (Eocene subduction) and Middle Miocene to Pliocene (Palawan subduction), respectively (modified from Soeria-Atmadja *et al.*, 1999). The ternary diagram is the QFL grouping of the Middle-to-Late Miocene mineralogy in the study area.

M33 marker) moderately quartzose sandstones (Tanean *et al.*, 1996; Soeria-Atmadja *et al.*, 1999), where most of the lithic content is from the sedimentary and metamorphic-rock particles (Werdaya *et al.*, 2017). Going up to ples (M65M50) have the highest quartz (the average of >80%) but oppositely have the lowest feldspar and lithic compositions (Figure 5). In summary, the rock samples in this study exhibit a turtle-shaped trend that goes from

the lowermost part of Middle Miocene (M40M33) with the low-quartz content but high in rigid materials (feldspar and lithics). It gradually changes into the majority of the Middle to Late Miocene rock samples that show higher-quartz content but low in rigid materials. And interestingly, the uppermost part of Late Miocene had inspired this study's hypothesis that there must have been long but sufficient processes of sediment transport and its sedimentation through the drainage systems of the proto-Mahakam's deltaic (Kutei Basin) towards the deep-water settings at the North Makassar Basins (Figures 3 and 4).

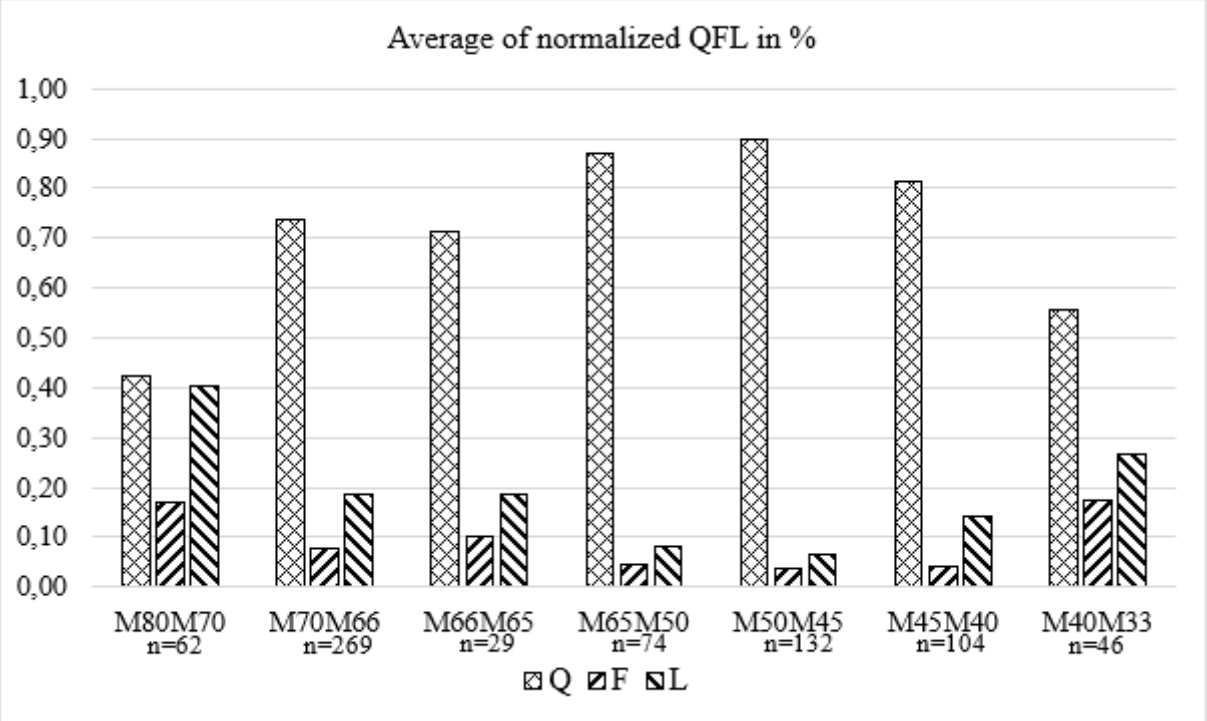

Figure 5. A bar graph showing the average composition of normalized QFL grains from the earliest Middle Miocene (M40M33) to the upper part of Late Miocene (M80M70).

(M80M70) is nearly similar to the composition of the M40M33's rock samples (Figure 5).

DISCUSSIONS

This study observes the QFL classification of the onshore and offshore samples, but mainly focuses in predicting the unpenetrated Middle Miocene's deep-water sandstones. To be compared with the existing deep-water's producing sandstones, this study includes the Late Miocene's rock samples. The highest sedimentation rate of the Kutei and outboard Sabah Basins was indicated in the middle to late Miocene as the result of Sabah uplift and erosion (Hutchinson, 2005; *in* Morley *et al*., 2016), and is potentially able to deliver huge clastics materials into the paleo deep-water slope of the north Makassar Basin through the incised valleys (IV) and slump scars trending parallely to the anticline of Tunu Field (Yoga *et al*. 2009 *in* Nugrahanto *et al*., 2021). This huge sedimentary mass initiated the gravitational flow to form the toe-thrust fold belt in the distal part of the system (McClay, 2000). These references This study pays more attention to lowstand and highstand system tracts (LST and HST) that enable periodic sub-regional incisions and / or collapses along the marine-shelf edge. Forced regressions that responded to the relative sea-level fall were observed by well and seismic data onshore and offshore (Nugrahanto *et al*., 2021). These events were indicated by the increase in sedimentation rates with significant shelf-break progradation at the northern and southern parts of the Kutei Basin during the deposition of M40M45 intervals. Decreasing of the sedimentation rates took place at the lower part of the M45M50, and had reached the lowest rate at the top most of the M50 before the rate was back to increase towards the top of M65 marker. These dynamic process of Middle Miocene deposition had subdivided drainage clusters of the Kutei Basin into north and south (Figure 3).

Middle Miocene's Mineralogy, Litho Facies, and Reservoir Quality

The Middle Miocene's rock samples are taken from around thirty wellbores located onshore. The deposi-

tional environment of the sandstone reservoirs is divided into fluvial-deltaic plain channels and delta-front bars. The sandstone's litho facies is further subdivided into four classifications: 1) cross-bedded fluvial sandstones (FLU_SX and DC_SX), 2) massive distributary channels (DC_SM), 3) bioturbated distributary channels (DC_SB), 4) bioturbated with mud/clay drapped bars (DF_SC). These are illustrated in the Figure 6, as well as the detailed core-description, core photos, and well-log types (modified from Butterworth *et al*., 2001; Lambiase *et al*., 2017; Riadi *et al*., 2018).

Figure 7 demonstrates the best quality of sandstone's litho facies are dominated by FLU_SX of both M50M45 and M45M40 sections, while small part of this category is represented by the litho facies DC_SX of M50M45 and DF_SC of M45M40. The detailed description of these litho facies characterized by upper medium- to lower coarse-grained sublitharenite sandstones that have cross-bedding structures, overall blocky to upwards fining succession, but relatively massive textures (non-laminated), moderately to well sorting, subangular to subrounded grains, none to traces porefilling cements/ overgrowth of quartz (<1.5%), carbonate (<10% siderite), and clay materials (<5% of kaolinite).

Common sedimentary structures associated with concretion-rich layers are parallel laminae and trough cross-bedding with high-energy that closely relate to insignificant fall of relative sea level. The other high-energy features are illustrated by planar and trough cross beddings (Chiarella & Longhitano, 2012, Longhitano *et al*.,2014 both *in* Ghaznavi *et al*., 2019). The coarse-grained sediments suggest a range of moderate to high energy depositions (Boggs, 2009; *in* Ghaznavi *et al*., 2019), while the well-sorted and subrounded grains are devoid of matrix, also indicating a high-energy beach subenvironment (Ghaznavi *et al*., 2019). The low-carbonate cements had usually been observed in the high-energy deposition like the distributary channels (Werdaya *et al*., 2017). These references suggest the FLU_SX, DC_SX, and DF_SC of the Middle Miocene (M50M45 and M45M40) sandstone's litho facies had been associated with the high-sedimentation rate (Morley *et al*., 2016; shown in the Figure 2), which might potentially be related to the relative sea-level fall (Nugrahanto *et al*., 2021).

In contrast to the best sandstone reservoir aforementioned, the bottom-left corner of Figure 7 displays the poor quality of sandstone's litho facies DF_SC (M45M40), DC_SX (M50M45 and M65M50), FLU_SX (M50M45), and DC_SB (M50M45). This category reflects high variation in the litho facies, however the most distinctive aspects that set them into poor quality are mixed medium-to fine-grained and mainly laminated sandstones with more pore filled with cements such as calcite and dolomites (trace – up to 10%), and quartz (1.5% - 8%), in addition to the siderite and kaolinite within the best reservoir quality. This study also observed the increase of rigid materials (feldspar and lithics). However, normalized lithics incremental of >10% - up to 30% looks more significant than the feldspar, which are both higher than the one at best-quality sandstone's litho facies.

Ahmad *et al*. (2013 *in* Ghaznavi *et al*., 2019) found that a low-energy environment is represented by the gypsiferous shale and siltstone to sandstone facies. Werdaya *et al*. (2017) suggested the Early Miocene sandstones are mainly composed by ductile to rigid detrital minerals associated with low-energy of deposition, which may potentially be sensitive to the depth of burial. Likewise, the porosity of the sandstones dramatically reduce to <5% when the carbonate cement exceeds >6%, and the permeability down to 0.1 mD to become non-reservoir rock. In line with these citations, the increase of burial depth in the study area may damage the DF_SC, DC_SX, FLU_SX, and DC_SB litho facies even if they were medium-grained sandstones. Along with the depth of burial aspect, higher quartz cement would definitely reduce these litho facies into none reservoir quality; in particular the DF_SC litho facies that demonstrate <5% core porosity and <0.1 mD core permeability (Figure 7).

The ternary diagram in Figure 6 shows five group of rock samples: (a) the samples from LR and PA wells demonstrate the older strata (M40M33) in the southern drainage system is dominated by the shallow-marine sandstones. They have dominant lithic arkose to feldspathic litharenite classification. (b) The remaining M40M33 samples from NA, NB, and P wells in the northern drainage are mainly sublitharenite to litharenite composition. The decreasing of feldspar and lithic contents in the younger strata of M45M40 can be subdivided into two sub classifications: (c) a wide range from sublitharenite, feldspathic litharenite, and litharenite at the SE and P wellbores representing the northern drainage, and (d) subarkosic dominant as shown in the samples from PR and PA wells representing the southern drainage. (e) The uppermost Middle Miocene samples of M50M45 have less feldspar and lithic contents than the previous two intervals at both the northern (NA and NB wells) and the southern (MA and MB wells) drainages.

The ternary diagram in Figure 8 shows the opposite trend from the older (M65M50) to the younger

(M80M70) sections, where (a) to (d) reflects the decrease of quartzarenite and sublitharenite compositions to become more feldspathic litharenite and litharenite.

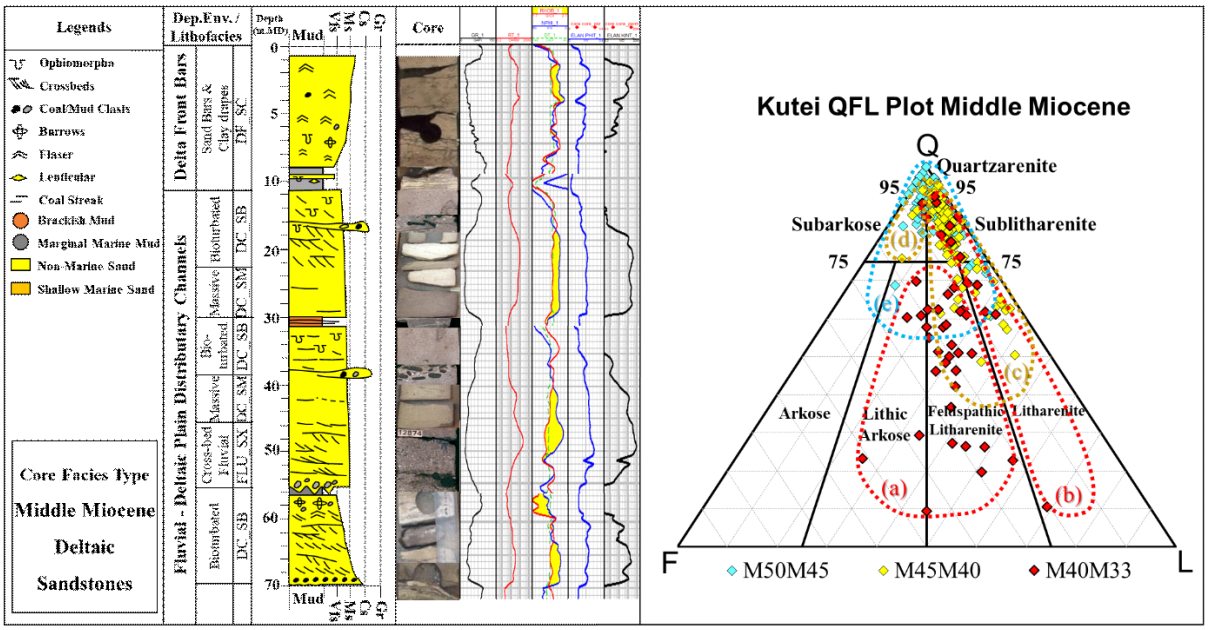

Figure 6. Core-facies Type of the Middle Miocene deltaic sandstones (modified from Butterworth *et al*., 2001; Lambiase *et al*., 2017, and Riadi *et al*., 2018), along with their QFL grouping in the ternary diagram.

It is important to notice that the best sandstone's litho facies of FLU_SX commonly has blocky and / or upwards fining (bell-shaped) GR-log. Contrarily, the poor sandstone's litho facies of DF_SC, DC_SX, FLU_SX, and DC_SB are various in the well-log types due to mixed descriptions of grain size (fine to medium), depth of burial, and cementations. The lowest core porosity and permeability values are mainly observed in the DF_SC litho facies that usually has upwards coarsening (funnel-shaped) GR log (Figures 6 and 7).

Late Miocene's Mineralogy, Litho Facies, and Reservoir Quality

The Late Miocene's samples from ten wellbores located offshore have been evaluated in order to characterize the depositional environment of the sandstone reservoirs. It is noteworthy most of these rock samples do not reach the lowest part of the Late Miocene (M65M50) interval except three wellbores in the northern drainage. Regrettably, there have been none of conventional core data representing the deep-water slope to basin floor settings in the M65M50. Therefore, this study refers to Saller *et al*. (2008) who had described the core data of Gendalo Late Miocene 1020 sandstone (7–8 Ma). This is equivalent to the M70M66 marker, which is associated with the highest sedimentation rate or maximum progradation throughout the Kutai Basin (Figure 2). The coherency attribute from 3-D seismic data (Saller *et al*., 2008) and regional isopach map (Nugrahanto *et al*., 2021) had defined the northwestern feeder system as the source of sediments for the deep-water slope fans in this specific area.

There are four litho facies had been reported is Saller *et al*. (2008): 1) High net-to-gross (NTG) ratio of 65%-100% sand, called Ta – the fine-grained massive sandstone with good porosity (20%-30%) and permeability (100-2,000 mD) that has an average individual sand beds of <1.0 feet, but rarely amalgamated. 2) Medium NTG ratio of 30%-65% sand, assigned Tb and Tc – the Tb is fine-grained and parallel laminae sandstone with coal-organic matters; while the Tc is very fine-grained rippled sandstone. 3) Low NTG ratio of 10%-30% sand (Tc); and 4) Non-reservoir with NTG ratio of <10%, which are mainly shale and debrites (Figure 8). The sandstones are generally dark color as they comprise abundant carbonaceous-organic matters that are commonly revealed within the parallel-laminated sandstones (Tb); Saller *et al*. (2006 *in* Saller *et al*., 2008).

This study had observed deep-water's litho facies in relationship with their reservoir quality; as shown at Figure 9: (i) a group of high porosity (>22%) with moderate (>35 mD) to high (>100 mD) permeability, which is predominantly well-sorted, fine to medium-grained sandstones; (ii) another group of moderate porosity (17%-22%) with moderate (>11-100 mD) to high permeability (>100 mD) that shows well-sorted, fine-grained sand-

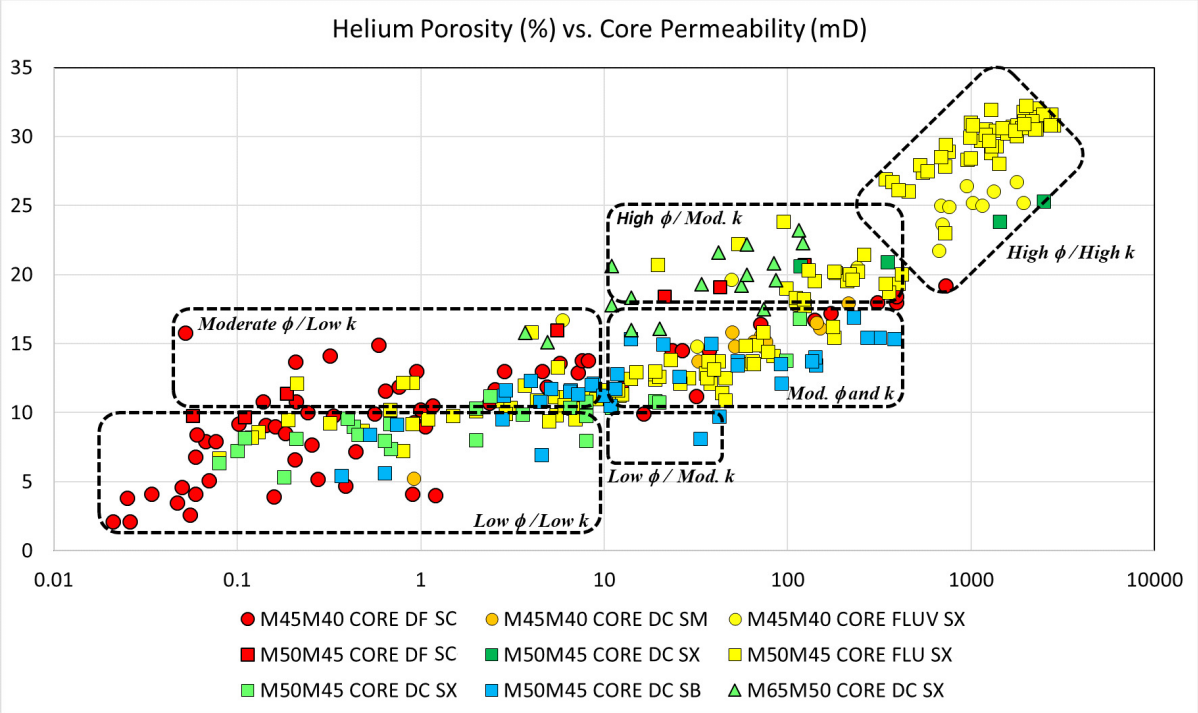

Figure 7. A cross plot of core-porosity vs. core-permeability in relation to the sandstone's litho types in the Middle Miocene section.

stone. Both group (i) and (ii) are mainly well-sorted sandstones (SSWS) with minor exception from medium-grained, poorly-sorted sandstones (SSPS) that have negligible clay matrix, but slightly high cements (>10%); and from fine- to medium-grained, poorly-sorted muddy sandstone (MSPS) that contains low clay matrix (none to <15%) and low cements (<6%). The last group (iii) is low to moderate porosity (up to 26%) with low permeability (<11 mD) poorly sorted sandstone (SSPS), and poorly sorted muddy sandstone (MSPS) with little anomaly from well sorted sandstone (SSWS) and well-sorted muddy sandstone (MSWS); where all containing high-clay matrix of >16% - up to 50%. Important to note the core porosity and permeability data @ambient condition is selected to represent more samples (than @overburden condition) since the difference of both conditions are considerably small; 1% to 4%.

Aligning the NTG-based (Saller *et al.*, 2008) and sorting-based (this study, 2021) of the deep water's lithofacies grouping, conclude that high-NTG ratio is closely related to well-sorted sandstone litho facies; while lower NTG-ratio is associated with poorly-sorted sandstone litho facies.

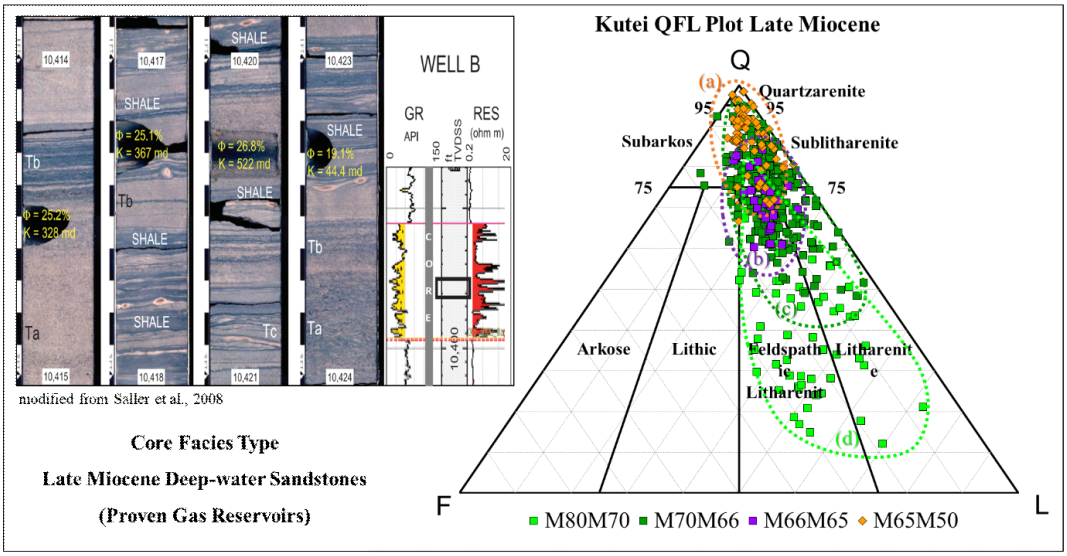

Figure 8. Core-facies Type of the Late Miocene deep-water sandstones (modified from Saller *et al.*, 2008) with the ternary diagram showing the QFL grouping of the Late Miocene interval.

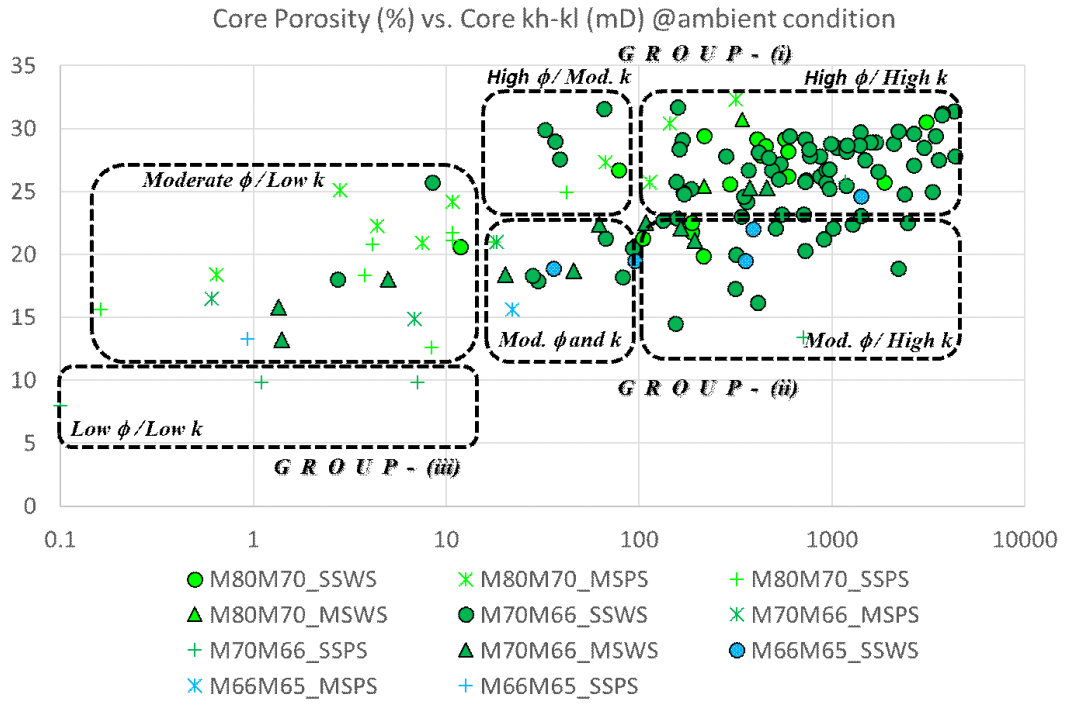

Figure 10. A cross plot of core-based helium porosity (%) versus the maximum burial depth (in feet), which is below mudline (bml) for the offshore wellbores. The circles are the Late Miocene, while the square ones are the Middle Miocene's rock samples data point.

The overall samples in the Late Miocene stratas have negligible arkosic content and predominantly litharenitic as seen on the right hand side of the ternary diagram. Opposite to the Middle Miocene's QFL trend, the Late Miocene's shows incremental lithic but reduction in quartz contents toward the younger strata from M65M50 (a) to M80M70 (d) strata (Figure 8).

Predicting the Reservoir Quality

Relational trends of the core-based porosity with maximum-burial depth and their associated litho facies are illustrated in the Figure 10. The rock samples are from conventional core data in the wellbores located onshore and offshore where the circles are the Late Miocene's deep-water facies, and the squares are the Middle Miocene's deltaic facies data point. Three permeability cut-off trends are plotted to classify the quality of reservoirs, which have been divided into none-poor (<10 mD), moderate-good (10-100 mD), and excellent (>1000 mD) reservoir quality. As discussed earlier, the Middle Miocene's deltaic FLU_SX, DC_SX, and DC_SM litho facies represent the excellent reservoir quality, while the DF_SC litho facies dominates the none-poor ones. The excellent reservoir quality of the Late

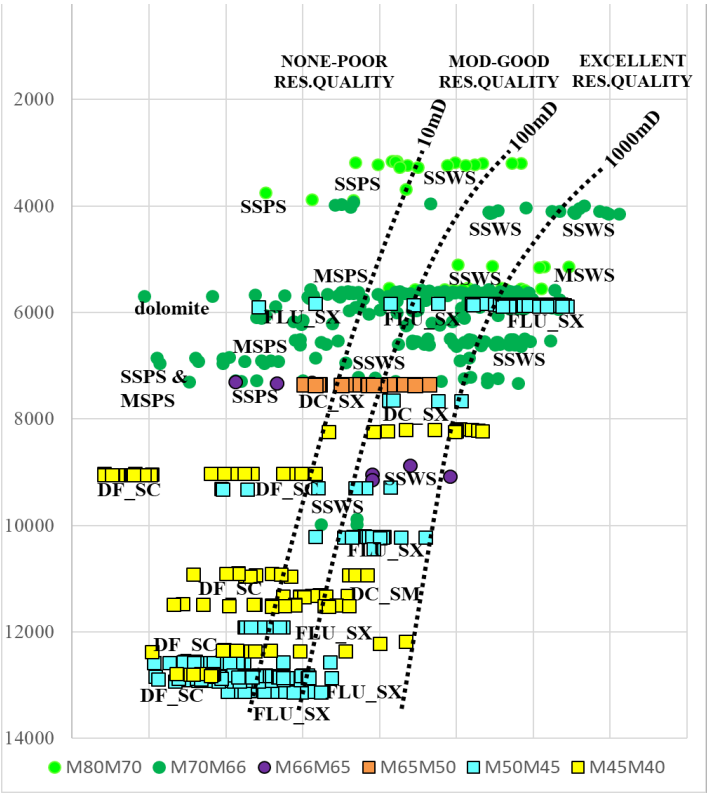

Figure 10. A cross plot of core-based helium porosity (%) versus the maximum burial depth (in feet), which is below mudline (bml) for the offshore wellbores. The circles are the Late Miocene, while the square ones are the Middle Miocene's rock samples data point.

Miocene's deep-water reservoir has been dominated by the SSWS lithofacies, while the none-poor ones are portrayed by the SSPS and MSPS litho facies.

The cross plot of the core-based porosity versus depth in Figure 10 shows a general trend of decreasing porosity with increasing of depth. One thing that stands out most when the decrease of core-based permeability's trend line with depth is not as much as the other two permeability trend lines. It is clearly seen that the reservoir's litho facies of clean (low clay matrix and cements), fine to medium-grain size, and well sorting is able to maintain its quality against the depth of burial.

Comprehensive seismic and well-based GDE mapping is considerably very important to assess and locate the litho facies variation especially the ones associated with the high-energy deposition. Extracting the litho facies information from the GDE map would be able to predict the porosity and permeability of the unpenetrated Middle Miocene's deep-water reservoirs.

CONCLUSIONS

The Middle to Late Miocene (M40 to M70 markers) rock samples reveal a strong correlation between the high quartz and low feldspar-lithics trend with the high peaks of sedimentation-rate package, which is much higher than any peaks within the Late Miocene to the modern-day Mahakam. The proto Mahakam River has been widely considered as the Neogene's drainage systems that delivered most of the sediments toward the Kutei and North Makassar basins. Thicker isopach provided paleo-drainage systems of either incised-valley fill and / or sedimentary pods in the deltaic to marine-shelf settings, and led the potential high-energy deposition of clastic-reservoirs further into the deep-water slope and basin floor settings.

Contrarily to the M40 to M70 interval, low-quartz but high content in rigid materials (feldspar and lithics) are exhibited in the rock samples from the onshore wellbores of the older Middle Miocene (M40M33) to Early Miocene (M33 and older), as well as the uppermost part of Late Miocene (M80M70). The M40M33 in the southern-drainage system is dominated by lithic arkose to feldspathic litharenite, while the rock samples in the northern drainage are mainly sublitharenite to litharenite composition.

The Middle Miocene FLU_SX deltaic litho facies that commonly has upwards fining (bell-shaped) to blocky GR-log is identified the best reservoir quality among the rock samples from the onshore wellbores. The Middle Miocene DF_SC, DC_SX, DC_SB, and even the FLU_SX deltaic litho facies are observed poorer in reservoir quality due to huge variation in finer grain size, depth of burial, as well as the carbonate cementation. The upwards coarsening (funnel-shaped) GR log of DF_SC litho facies is commonly found the worst in reservoir quality.

In the absence of deep-water facies rock samples; especially the conventional core data from the Middle Miocene age, this study has classified the Late Miocene's deep water litho-facies into groups and found the alignment between NTG-based with the sorting-based litho facies. It summarizes that the best deep-water sandstone reservoir has high-NTG ratio and good sorting, while oppositely the lower NTG-ratio and poorly-sorted ones represent the worst reservoir quality. The Late Miocene rock samples reveal negligible arkosic with predominantly litharenitic contents, and exhibits the increase in lithic but reduction in the quartz contents toward the younger strata from M65M50 (a) to M80M70 (d) strata.

The litho facies of fine-to medium-grained, and well-sorted sandstone reservoirs that contain negligible-to-low clay matrix and cements would be able to preserve its quality against the burial depth. The cross plot exhibits the decrease of the excellent permeability's trend line with depth is not as aggressive as the other two permeability trend lines. The GDE mapping is very essential to afford the important information of the litho facies that go along with the high-energy deposition, which may be able to provide the excellent reservoir quality.

ACKNOWLEDGEMENTS

The authors would like to thank the Faculty of Geological Engineering of the University of Padjadjaran (Unpad), as well as the Centre of Data and Information Technology (Pusdatin), which is under the Ministry of Energy and Mineral Resources (ESDM) of Indonesia. The supporting data from, and the technical consultation with the Exploration New Ventures Team at Upstream Subholding Pertamina Hulu Energi (PHE SHU), Pertamina Hulu Sanga Sanga (PHSS), Pertamina Hulu Kalimantan Timur (PHKT), and Pertamina Hulu Mahakam (PHM) have been really constructive. Without all of these continuing supports, this study would have not been completed. Our gratitude is also conveyed to every parties whose contribution were significant in this study, which is Kuntadi Nugrahanto's thesis at the magister program of Unpad. This study is the authors' personal view hence do not represent all the above-mentioned organizations.

REFERENCES

Advokaat, E.L., Marshall, N.T., Li, S., Spakman, W., Krijgsman, W., and van Hinsbergen, D.J.J., 2018.

Cenozoic Rotation History of Borneo and Sundaland, SE Asia Revealed by Paleomagnetism, Seismic Tomography, and Kinematic Reconstruction. *Tectonics July 2018*, p.1-27.

Baryati, F. D., Setiawan, T., Meilany, Y., Assalam, A., 2019. The Progressive Illitization Process, Diagenetic Mechanism and Its Effect on Reservoir Quality Based On SEM, Burial History, and Simultaneous Multi-Well Analysis: A Case Study in The Sanga-Sanga Block, Kutai Basin, East Kalimantan. *Proceedings Indonesian Petroleum Association 43rd Annual Convention and Exhibition, October 2019*.

Butterworth, P.J., Cook, P., Dewanto, H., Drummond, D., Kiesow, U., McMahon, I.T., Ripple, R.A., Setoputri, A., and Sidi, F.H., 2001. Reservoir Architecture of an Incised Valley-fill from The Nilam Field, Kutai Basin, Indonesia. *Proceedings Indonesian Petroleum Association 28th Annual Convention and Exhibition, October 2001*.

Corelab, 2003. Kutei Basin Regional Evaluation, Chapter 6: Reservoir Quality, Section 6.3: Petrographic Analysis of Diagenetic Effects. Internal Report of Unocal Indonesia, unpublished.

Duval, B.C., de Janvry, G. C., Loiret, B., 1992. *Offshore Technology Conference*, 4-7 May, Houston, Texas.

Ghaznavi, A. A., Quasim, M. A., Ahmad, A. H. M., Ghosh, S. K., 2019. Granulometric and facies analysis of Middle-Upper Jurassic rocks of Ler Dome, Kachchh, western India: an attempt to reconstruct the depositional environment. *Geologos 25, 1 (2019)*: 51-73.

Hall, R. and Sevastjanova, I., 2012. Australian Crust in Indonesia. *Australian Journal of Earth Sciences*, 59: 827-844).

Hall, R., 2013. The Palaeogeography of Sundaland and Wallacea Since the Late Jurassic, *J. Limnol.*, 72(s2): 1- Geological History. DOI: 10.4081/ jlimnol.2013.s2.e2

Heins, W. A., Kairo, S., 2007. Predicting sand character with integrated genetic analysis. *Geological Society of America Special Papers 2007*; 420; 345-379. DOI:10.1130/2006/2420(20) downloaded from specialpapers.gsapubs.org on June 22, 2015.

Lambiase, J. J., Riadi, R. S., Nirsal, N., Husein, S., 2017. Transgressive successions of the Mahakam Delta Province, Indonesia. From: Hampson, G. J., Reynolds, A. D., Kostic, B. & Wells, M. R. (eds) 2017. Sedimentology of Paralic Reservoirs: Recent Advances. *Geological Society, London, Special Publications, 444*, 335 –348.

McClay, K., Dooley, T., Ferguson, A., and Poblet, J., 2000. Tectonic Evolution of the Sanga Sanga Block, Mahakam Delta, Kalimantan, Indonesia. *The American Association of Petroleum Geologists (AAPG) Bulletin*, 84(6): 765-786.

Metcalfe, I., 2011. Tectonic Framework and Phanerozoic Evolution of Sundaland. *Gondwana Research*, 19: 3-21.

Metcalfe, I., 2013. Gondwana Dispersion and Asian Accretion: Tectonic and Palaegeographic Evolution of Eastern Tethys. *Journal of Asian Earth Sciences*, 66: 1-33.

Morley, J.M., Morley, H.P., and Swiecicki, T., 2016. Mio-Pliocene Palaeogeography, Uplands and River Systems of the Sunda Region Based On Mapping Within A Framework of VIM Depositional Cycles. *Proceedings, Indonesian Petroleum Association 40th Annual Convention and Exhibition, May 2016.*

Moss, S.J., Chambers, J., Cloke, I., Satria, D., Ali, J.R., Baker, S., Milsom, J., and Carter., 1997. New Observation on the sedimentary and tectonic evolution of the Tertiary Kutai Basin, East Kalimantan. *in* Fraser, A. J., Matthews, S. J., and Murphy, R. W. (Eds.). *Petroleum Geology of Southeast Asia*. Geological Society Special Publication, 126: 395-416.

Nugrahanto, K., Syafri, I., Muljana, B., 2021. Depositional Environment of Deep-Water Fan Facies: A Case Study of the Middle Miocene Interval at the Kutei and North Makassar Basins. *Journal of Geology and Mineral Resources*, Vol. 22. No. 1 Februari 2021 hal 45-57.

Riadi, R. S., Permana, R. C., Setoputri, A., Andaryani, S., 2018. Fresh Outlook of Reservoir Understanding and Implication for Further Development Strategy of Mature Fields, Case Study from Semberah and Mutiara Fields, Kutei Basin, Indonesia. *Proceedings: Indonesian Petroleum Association 42nd Annual Convention and Exhibition, May 2018.*

Saller, A.H., and Vijaya, S., 2002. Depositional and Diagenetic History of the Kerendan Carbonate Platform, Oligocene, Central Kalimantan, Indonesia. *Journal of Petroleum Geology*, 25(2): 123-150.

Saller, A., Werner, K., Sugiaman, F., Cebastiant, A., May, R., Glenn, D., and Barker, C., 2008. Characteristics of Pleistocene Deep-water Fan Lobes and Their Application to an Upper Miocene Reservoir Model, Offshore East Kalimantan, Indonesia. *The American Association of Petroleum Geologists Bulletin*, 92(7): 919–949.

Shanmugam, G., 2013. New Perspectives on Deep-water Sandstones: Implications. *Petrol. Explor. Develop.*, 40(3): 316–324.

Shanmugam, G., 2015. Lithofacies Palaeogeography and Sedimentology - Submarine Fans: A Critical Retrospective (1950-2015). *Journal of Palaeogeography*, 5(2):110-184 (00095).

Shanmugam, G., 2017. Contourites: Physical Oceanography, Process Sedimentology and Petroleum Geology. *Petroleum Exploration and Development*, 44: 183–216.

Shuang Li, S., Yang, X., Sun, W., 2015. The Lamandau IOCG deposit, southwestern Kalimantan Island, Indonesia: Evidence for its formation from geochronology, mineralogy, and petrogenesis of igneous host rocks. *Ore Geology Reviews 68* (2015) 43-58.

Soeria-Atmadja, R., Noeradi, D., Priadi, B., 1999. Cenozoic magmatism in Kalimantan and its related geodynamic evolution. *Journal of Asian Earth Sciences 17 (1999),* 25-45.

Supriatna., S., Sukardi, and Rustandi, E., 1995. *Geological Map of Samarinda Sheet, 1:250,000*. Geological Research and Development Center, Bandung, Indonesia.

Tanean, H., 1994. Petrology and Provenance of the Miocene Sediments in the Kutai Basin, Appendix 8.1: Reservoir Studies – Hondiro Tanean. File/ Report No. GR.950601, Map No.: 1405-20. Virginia Indonesia Company (VICO), unpublished.

Tanean, H., Paterson, D. W., Endharto, M., 1996. Source Provenance Interpretation of Kutei Basin Sandstones and The Implications for The Tectono-Stratigraphic Evolution of Kalimantan. *Proceedings Indonesian Petroleum Association 25th Silver Anniversary Convention and Exhibition, October 1996.*

Werdaya, A., Alexandra, M., Nugrahanto, K., Anshori, R., Pradipta, A., Armitage, P., 2017. Comprehensive Evaluation of Reservoir Quality in the Early Miocene, Kutei Basin, Onshore East Kalimantan. *Proceedings Indonesian Petroleum Association 41st Annual Convention and Exhibition, May 2017.*

Witts, D., Davies, L., Morley, R., 2014. Uplift of the Meratus Complex: Sedimentology, Biostratigraphy, Provenance, and Structure. *Proceedings Indonesian Petroleum Association 38th Annual Convention and Exhibition, May 2014.*

Witts, D., Davies, L., Morley, J.M., and Anderson, L., 2015. Neogene Deformation of East Kalimantan: A Regional Perspective. *Proceedings Indonesian Petroleum Association 39th Annual Convention and Exhibition, May 2015*.